JMATPRO	Journal of Advanced Materials and Processing 11 (2): 3-14, Spring 2023 https://sanad.iau.ir/journal/jmatpro Doi: 10.71670/jmatpro.2024.981663

Research Paper

Fine Grain Formation in as Cold Worked SP700 Titanium Alloy and Its Effect on Mechanical and Superplastic Properties

Marjan Daryaban[1], Maryam Morakabati[2*], Nooshin Meraji[3]

1. MS. C., Department of Materials and Manufacturing Thechnologies, Malek Ashtar University of Technology, Tehran, Iran.

2. Associate Professor, Department of Materials and Manufacturing Thechnologies, Malek Ashtar University of Technology, Tehran, Iran.

3. MS. C., Department of Materials and Manufacturing Thechnologies, Malek Ashtar University of Technology, Tehran, Iran.

ARTICLE INFO

Article history:

Received 23 November 2023
Accepted 30 April 2024
Available online 1 May 2023

Keywords:
SP700 titanium alloy
Cold working
Dynamic recrystallization
Superplastic
Fundamental equations.

ABSTRACT

The aim of this research is to study the effect of fine grain structure on the mechanical and superplastic properties of cold worked SP700 alloy. Thickness reductions of 20%, 40%, and 60%. were applied during cold rolling. Then the specimens were annealed at 700°C, 750°C, and 800°C for 40 minutes. The tensile test was applied at 25, 700ºC, 750°C, and 800°C with strain rates of $0.01s^{-1}$, $0.005s^{-1}$ and $0.001s^{-1}$. The SEM and OM were used to analyze the specimens' microstructures. The alloy cold rolled to 40% reduction and annealed at 700°C exhibited a maximum elongation of 1380% at a stress level of 30 MPa and a strain rate of 0.005 s^{-1} at 700°C. Microstructural evlauation showed that during the superplastic test, dynamic recrystallization took place. The strain rate sensitivity varied in the range of 0.32 to 0.46. Fundamental equations were also used to determine the mechanism of superplasticity. The activation energy is obtained as 385 $kJ.mol^{-1}$. Results validated that the Rachinger sliding is the main superplastic mechanism in the SP700 alloy.

Citation: Daryaban, M.; Morakabati, M.; Meraji, N. (2023). Fine Grain Formation in as Cold Worked SP700 Titanium Alloy and Its Effect on Mechanical and Superplastic Properties, Journal of Advanced Materials and Processing, 11 (2), 3-14. Doi: 10.71670/jmatpro.2024.981663

* **Corresponding Author:**
E-Mail: m_morakabai@mut.ac.ir

1. Introduction:

Ti-4.5Al-3V-2Mo-2Fe, a dual-phase titanium alloy that performs better in terms of formability and workability than TC4 and Ti6Al4V alloys, is frequently used to create superplasticity [1, 2]. Due to its low flow stress and fine microstructure, which enable exceptional superplastic formability at 700 °C, Ti-4.5Al-3V-2Mo-2Fe is also known as SP700 [2]. This alloy's exceptional mechanical properties, heat treatability, and cold workability are all due to its fine microstructure [2]. Additionally, the three factors that increase the formability of titanium alloys are fine grain size; high temperature; and low strain rate. This causes an increase in production costs, which greatly reduces efficiency [3]. Complex-shaped parts used in different industrial sectors, such as aerospace, defence and automotive industries as well as biomedical and sport applications can be produced by exploiting the superplasticity of metals [4]. It is well known that titanium alloys can exhibit superplastic deformation under certain conditions [3, 5]. The superplasticity behavior of materials depends on the flow stress, the strain rate sensitivity, and the strain hardening exponent [6]. In titanium alloys, grain boundary sliding can also be addressed [3]. The grain boundary sliding, as well as diffusion, dislocation accommodations, and a combination of these two processes, regulate the superplastic mechanism in metal structures such as titanium, aluminum, and iron [7]. In dual-phase titanium alloys, α and β phases are stable structures. It has been reported that [3] the β phase with BCC crystallographic structre has more slip systems than the α phase with HCP crystallographic structre. Besides, the diffusion coefficient of β phas is higher than the α phase which is more responsible for deformation of titanium alloys than the α phase. This means that it is preferable to have higher volume fraction of the β-phase. However, with increasing the β phase, the grain growth is accelerated and grain boundary sliding diminished. As a result, the alloy with stable α/β phases and the best volume fraction and morphology of these phases has greater formability than the alloy with single β phase [8].

Studies on the superplastc properties of titanium alloys [7] indicate that their superplasticity and high elongation are due to the fine microstructure and the dynamic recrystallization. As reported by previous studies [9], grain boundary sliding and dislocation accommodation is the dominant superplastic deformation mode in Ti-6Al-4V alloy in the temperature range of 700–850°C. An earlier studyon the Ti-43Al-9V-0.2Y alloy [9] revealed that the elongation of 360% was achieved in the temperature range of 750-900 °C. In another research work [11], the superplastic deformation behavior of the Ti-6Al-4V alloy was applied using a theoretical model. The alloy showed an exceptional elongation of 790% and it has been reported that the deformation mechanism was based on dislocation migration. Ratochka et al. [12] examined the deformation-induced grains in ultrafine grained Ti–5Al–5V–5Mo–1Cr–1Fe alloy during superplastic deformation. They revealed that the formation of small grains between large grains leads to high elongation. The superplasticity behavior of Ti-4Al-3V-2Mo-2Fe alloy was assessed by Shen et al. [10]. They reported that the deformation of the alloy involved the combined effects of grain boundary sliding accommodated by dislocation movement, and dynamic recrystallization. They claimed that grain boundary sliding and dynamic recrystallization were responsible for the high superplasticity of this material at temperatures between 760 and 840 °C and strain rates between 0.03-0.3 s^{-1}.

In spite of various studies conducted on the superplastic deformation of SP700 titanium alloy, to the best of authors knowledge, the effect of cold working and subsequent annealing on the superplastic properties has not been carried out yet. Thus, the present work has been undertaken to enhance the superplasticity of the SP700 alloy by optimizing the cold working and heat treatment conditions. Thus the cold working was replaced by conventional hot working process. It should be noted that the applied strain during cold working has been changed. Furthermore, the subsequent annealing temperature as well as the test temperature and strain rate were varied.

2. Materials and Methods

2.1. Material preparation

The SP700 ingot with a length of 400 mm and a diameter of 120 mm was produced by Vacuum arc re-melting (VAR) method. The ingot was homogenized at 1100 °C for 3 hours and then air-cooled. The alloy was hot rolled into a plate with a cross section of 62 mm × 62 mm at this temperature, as well. Then, two steps of hot rolling was performed at 850 °C and the thickness of the plate decreased to 5.33 mm. After heat treatment of the received strip at 750°C, it was cut into three stirps. Subsequently, the strips were cold worked with thickness reductions of 20%, 40%, and 60%. To study the effect of annealing temperature on the microstructure and superplastic behavior of the alloy, the samples annealed at 700°C, 750°C, and 800°C for 40 min and then air cooled. Table 1 shows the chemical composition of the alloy, which is in the acceptable range for the SP700 alloy according to the AMS 4899 [11] and AMS 4964 [12] standards.

Table 1 . The Chemical composition analysis of the SP700 alloy (wt. %).

Alloy Element	Ti	Al	V	Mo	Fe
Limited Permitted according to the AMS 4899[14] and AMS 4964[15]	Balance	4-5	2.5-3.5	1.8-2.2	1.7-2.3
Ingot Analysis	89.15	4	3.00	1.8	2.16

The microstructure and superplasticity properties of the SP700 alloy were investigated in the following different conditions to obtain the strain rate and temperature at which the optimum superplasticity has been achieved.

1- Constant strain rate of 0.005 s^{-1} and different temperatures of 700, 750, and 800°C.

2- Constant temperature of 750°C and different strain rates of 0.01 s, 0.005, and 0.001 s^{-1}.

2.2. Evaluation of Microstructure and Mechanical Properties

The mechanical properties of the alloy was evaluated by performing tensile test at room temperature according to the ASTM E8M standard [13]. The superplastic test was performed at the temperature range of 700 to 800 °C with 50 °C intervals and strain rates of 0.001, 0.005, and 0.01 s^{-1}. The tests were performed using an Instron 8502 testing machine equipped with a resistance furnace. The microstructural observations were conducted using an OLYMPUS light microscope and a TESCAN-VEGA3 scanning electron microscope. The specimens were polished and etched with Kroll's reagent after grinding with 0.5 µm alumina powder. The Image J 1.44 analysis software used to measure the average grain size and the volume fraction of the phases.

3. Result and Discussion

3.1. Initial Microstructure of the SP700 alloy

Fig. 1 shows the microstructure of the alloy after secondary hot rolling at 850℃ and subsequent annealing at 750℃. The microstructure is characterized by elongated and equiaxed α phase distributed in the β matrix. The average grain size of α phase via the Image J 1.44 analysis software was obtained as 5.1 µm. The equiaxed α phase resulted from static spheroidization [14].

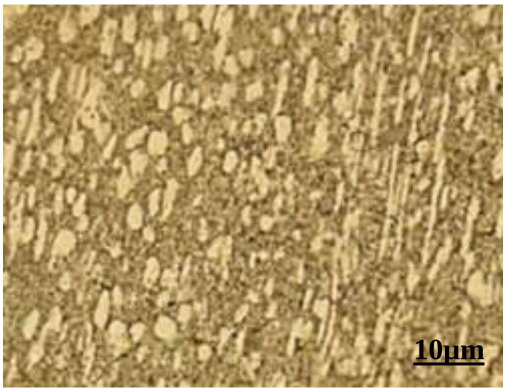

Fig. 1. The microstructure of the SP700 alloy after secondary hot rolling at 850℃ and subsequent annealing at 750℃.

In this study, cold rolling with various degrees of thickness reductions substituted for hot rolling to produce a lamellar structure in order to evaluate the positive effect of cold working and subsequent heat treatment in grain refining the microstructre, mechanical and superplastic behavior of the SP700 alloy. Each of cold rolled specimens with a thickness reductions of 20%, 40% and 60%, underwent to heat treatment at temperatures of 700℃, 750℃ and 800℃ for 40 minutes to obtain a desirable spheroidized structure along with the lamellar one.

3.2. Microstructure and tensile properties of the SP700 alloy after cold rolling

The microstructure of the SP700 alloy after cold rolling with thickness reductions of 20%, 40%, and 60% is shown in Fig. 2. The α phase with an average size of 3.11 µm and a thickness of 1.73 µm is observed in the β matrix in Fig. 2 (a). As the thickness reduction increases to 40% and 60%, the size of primary α phase increases slightly to 3.19 µm and 3.25 µm, and its thickness reduces to 1.05 µm and 0.6 µm, respectively showing the development of layered structure. During rolling, the α phase change its shape in a manner that corresponds to the macroscopic shape change. Therfore, the surface area of α phase is increased by increase in thickness reduction. The retention of contiguity of α phase and β phase requires that the new grain boundary area of α phase formed during deformation. This is done by the incorporation of the dislocations generated during rolling [12]. Hence, the microstructure of the 40% cold rolled specimen exhibits a mixture of spherical and lamellar α phase; However, the 60% cold rolled specimen contains fully lamellar α phase.

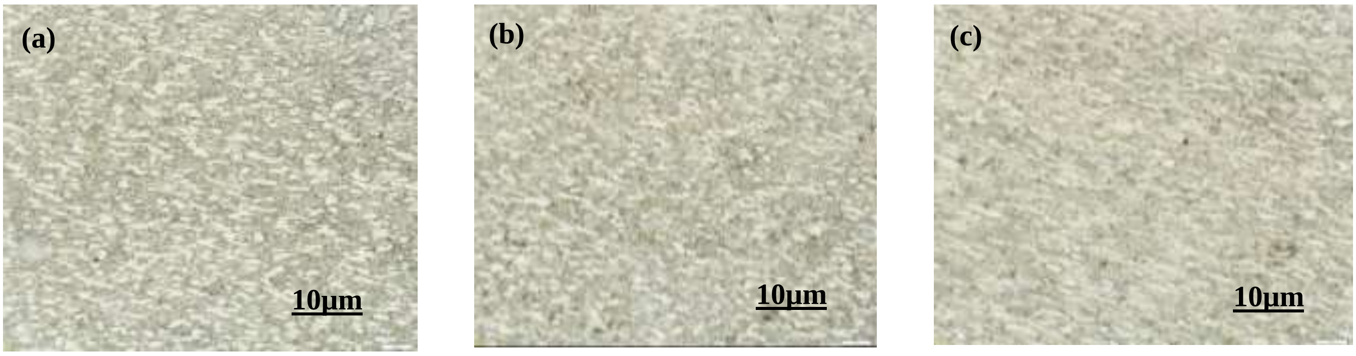

Fig. 2. The OM microstructur of the SP700 alloy after cold rolling with thickness reductions of; a) 20, b) 40 and , c) 60% .

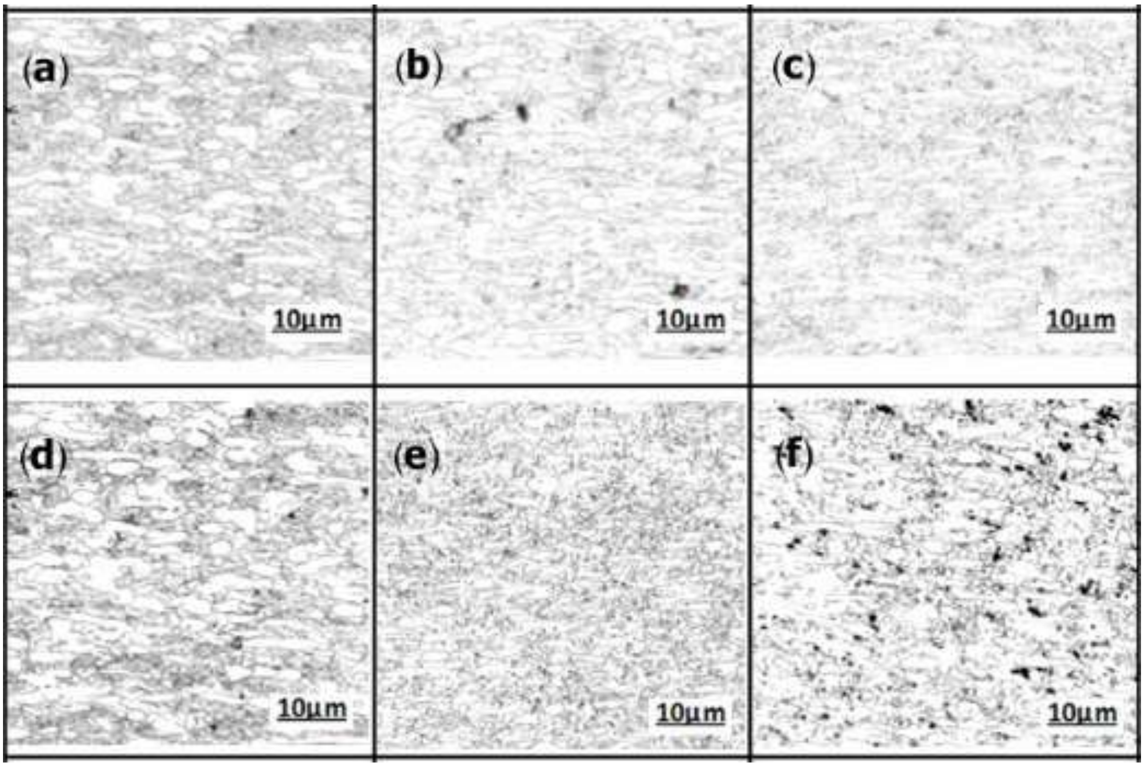

Fig. 3. The microstructure of the SP700 alloy after cold rolling with thickness reductions of a)20% , b) 40% and 60% and subsequently heat treatment at 700℃, and thickness reductions of d) 20% e) 40% and f) 60% and subsequently heat treatment at 750℃.

3.2.1. Microstructures of the SP700 alloy after heat treatment

The microstructure of the SP700 alloy after heat treatment at 700℃, 750℃ and 800℃ are shown in Fig. 3.

The mean size of the α phase in the 20% cold-rolled specimens heat treated at 700°C and 750°C was obtained as 2.83µm and 2.43 µm, respectively. Similarly, for the 40% cold-rolled specimens heat treated at the same temperatures, the dimonsion of the α phase was 3µm and 2.67µm, respectively. This was obtained for the 60% cold-rolled and heat treated specimens as 2.9 µm and 2.45 µm, respectively. As seen, the specimens heat treated at 700 and 750°C exhibited a microstructure with spheroidized α phase which were much smaller than the requirement of 10 µm for superplasticity [15]. As the temperature of heat treatment rises, the lamellar α phase decomposes and its spheroidization developed in the microstructure. The results show that the increase in the heat treatment temperature from 700 to 750 ºC reduces the size of α phase which confirms the development of static recrystallization or spheroidization.

As the thickness reduction during rolling enhances the increase in dislocation density, static recrystallization after the heat treatment and dynamic recrystallization facilitats during the test. It has been mentioned before that recrystallization and grain size are essential factors for achieving superior superplastic properties. Lamellar α phase formed during rolling provides preferential sites for recrystallization. This enhances the superplasticity of the alloy.

3.2.2. The room temperature mechanical properties after heat treatment

Fig. 4 shows the variation strength and ductility of the specimens cold-rolled up to 20%, 40%, and 60% and heat treated at 700°C and 750°C. As seen, the highest yield strength and ultimate tensile strength were obtained for the specimens cold-rolled with thickness reduction of 40% and heat treated at 700°C, which were 960 MPa and 1019 MPa, respectively.

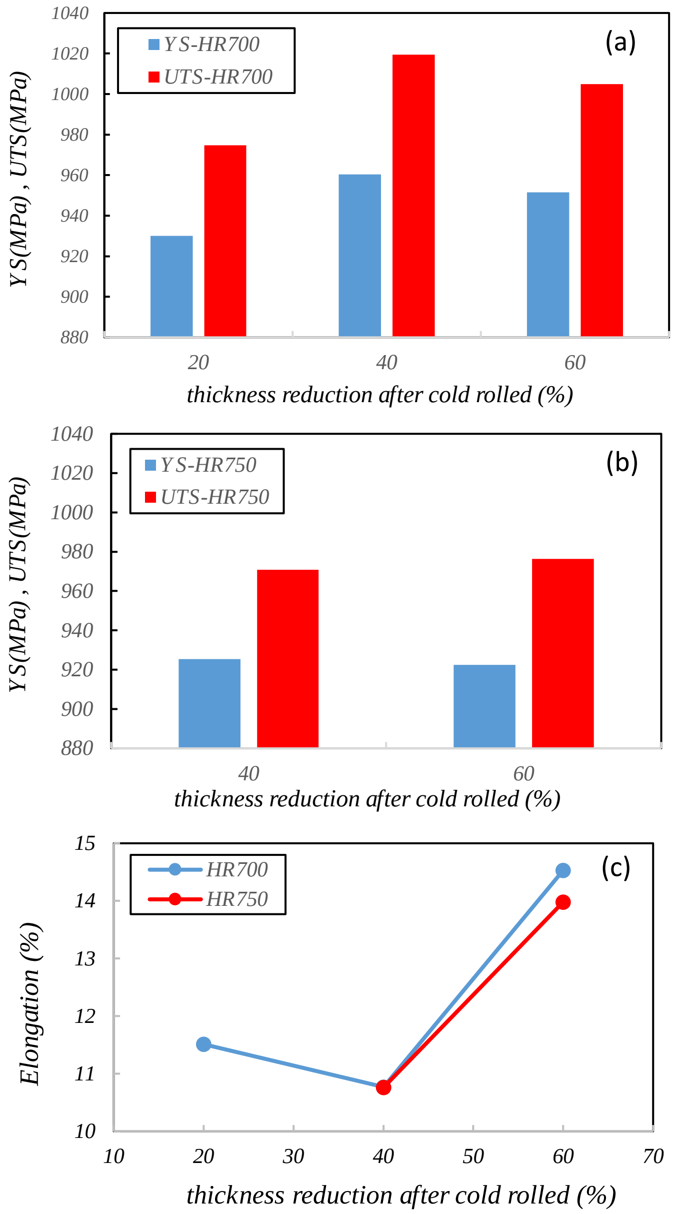

Fig. 4. The room temperature mechanical properties of the SP700 alloy: a) YS and UTS after heat treatment at 700°C, b) YS and UTS after heat treatment at 750°C, and c) Elongation after heat treatment at 700°C and 750°C.

3.3. Superplasticity of the SP700 alloy after heat treatment

To determine the optimal superplasticity and mechanical properties of the alloy after cold rolling with thickness reductions of 20%, 40% and 60%, and heat treatment at temperatures of 700°C, 750°C and 800°C, the superplastic test was conducted at a constant temperature of 800°C and a strain rate of $0.005s^{-1}$. Fig. 5 shows the image of the specimens after cold rolling and heat treatment at different conditions and constant condition of superplastic test. As seen, the specimens exhibited high uniform elongation without necking. Besides, the maximum elongation was achieved in the specimen cold rolled by 40% and heat treated at 700°C.

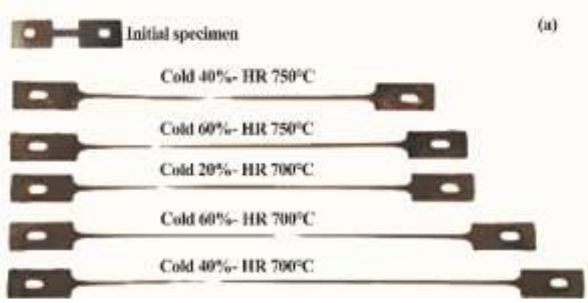

Fig.5. The image of the specimens after the superplastic test at 800 °C and strain rate of 0.005 s^{-1} at different conditions of cold rolling and heat treatment.

Fig. 6 illustrates the stress-strain curve of the SP700 alloy after superplastic test at a temperature of 800 °C and strain rate of 0.005 s^{-1}. As shown, the peak stress for the specimens at various conditions of cold rolling and heat treatment is approximately similar and is around 40MPa. This suggests that heat treatment does not significantly influence the maximum stress of the material during the superplastic test. It can also be observed that after the elastic region, the flow curves show rapid work hardening to a peak and gradual flow softening followed by a long steady state region and final softening to failure.

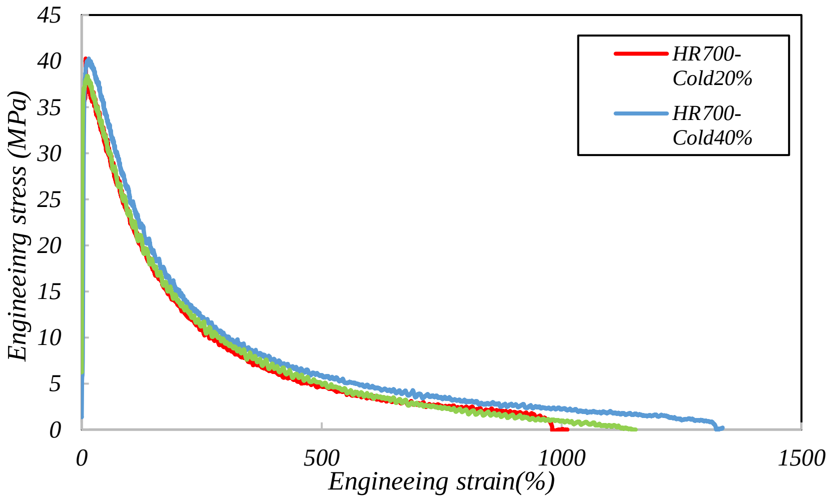

Fig. 6. The Stress- Strain curves of the alloy after superplastic test at 800 °C and strain rate of 0.005 s^{-1} (Condition of the specimens: cold rolling with different thickness reductions and heat treatment at 700ºC).

The elongations of the specimens cold rolled by thickness redutions of 20%, 40% and 60% and heat treated at 700°C were obtained as 980%, 1320%, and 1147%, respectively. The specimen cold rolled by thickness reduction of 40% and heat treated at 700°C, had the highest elongation.

Regarding to Figure 3, the thickness of lamellar α phase in the specimens cold rolled with thickness reductions of 20, 40, and 60% has been decreased as 1.73, 1.05, and 0.6 µm, respectively indicating the development of lamellar structure. Consequently, the average size of α phase in the 20%, 40%, and 60% cold rolled specimens after heat treatment at 700°C, were obtained as 2.83, 3, and 2.90 µm, respectively showing dynamic recrystallization. This shows that besides the grain size, other factors also influence the superplastic properties. The increase in dislocation density and consequently the development of lamellar structures are factors that affect the superplastic properties. As the layered structures are favorable sites for dynamic recrystallization, they improve the superplastic properties of the alloy as a consequence of grain refining. The increase in the area of grain boundaries as well as the dislocations density during cold deformation, are factors affecting the sequence of dynamic recrystallization of α phase and accelarte it. Therefore, as a consequence of diffuson of β phase into lamellar α plates, spherodized α phase with fine grain size developed in the microstructure leading to improvement in superplastic deformation for grain boundary sliding of fine spherodized α phase. The spherodization mechanism is mainly controlled by the migration of the triple junctions. This results in the fragmentation of the α lamella and the formation of new α/β boundaries. [16].

Fig. 7 displays the SEM microstructure of the specimen cold rolled with thickness reduction of 40% and heat treated at 700°C before and after superplastic test at 800 °C and strain rate of 0.005 s^{-1}. The microstructure of the specimen before the test exhibits the lamellar α phase with avearge length of 6.8 µm in β matrix (see Fig. 7.(a)). However, as shown in Fig. 7. b after the superplastic test, the semi-spherodized α phase with average size of 3.23 µm exhibited in the β matrix due to the accomplishment of dynamic recrystallization by applying stress during the test. Therefore, the findings of this study revealed that the optimal superplastic behavior is obtained when the spherodized α phase as well as lamellar α phase presented in the initial microstructure of the alloy.

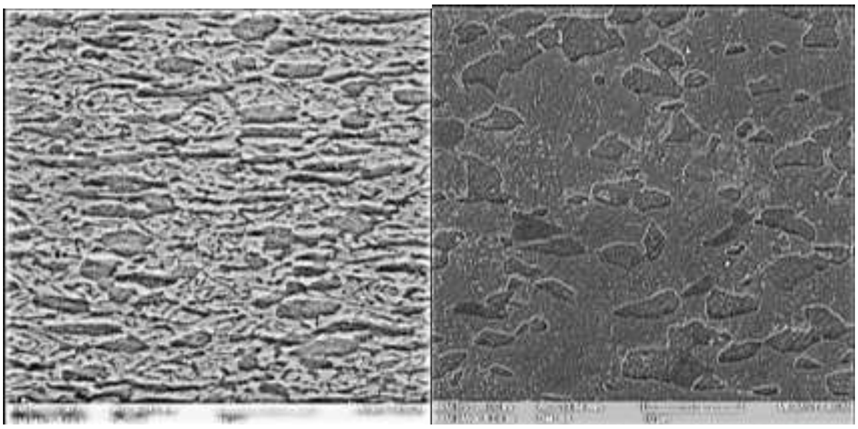

(a) (b)

Fig. 7. The specimen cold rolled with thickness reduction of 40% and heat treated at 700°C (a) before and (b) after superplastic test at 800 °C and strain rate of 0.005 s^{-1}.

As shown in Fig. 7, after the superplastic test, the percentage of the β phase has increased. The volume fraction of α and β phases after the superplastic test were obtained as 28.4% and 71.6%, respectively. While the volume fraction of α and β phases before the superplastic test was obtained as 58.5% and 41.5%, respectively. This is attributed to deformation of the alloy near the β transus temperature of it. It has been reported that [19], in the α/β titanium alloys, there are three kinds of boundaries: boundaries between the α phase (α/α), boundaries between the β phase (β/β), and the interfaces between the α and β phases (α/β). The sliding resistance of the mentiod boundaries followed this order: $\alpha/\beta \ll \alpha/\alpha \approx \beta/\beta$. Therefore, grain boundary sliding mainly takes place at the interfaces between the α and β phases (α/β). Since the β phase with a body center cubic (BCC) structure had more active slip systems than the α phase with a hexagonal close-packed crystal (HCP) structure, the β phase could be considered as the "soft phase" underwent larger plastic deformation. Besides, the volume fraction of β phase increased as the strain increased, which could be explained by the α→β phase transformation during deformation. The tensile stress caused the β stabilizer elements to move from the α to the β phase, leading to the α→β phase transformation.

3.4. The effects of superplastic testing conditions on superplastic behavior

3.4.1. The effect of temperature on the superplasticity

As mentioned in previous section, the SP700 alloy cold rolled to 40% reduction and heat treated at 700°C had the excellent mechanical and superplastic properties. Therefore, this specimen was chosen for further experiments and the results of this study are based on them. The superplastic behavior of the 40% cold rolled and 700°C heat treated specimen was investigated via deformation at 700°C, 750°C, and 800°C with a constant strain rate of 0.005 s^{-1} to examine the effect of deformation temperature on the superplastic respons of the alloy.

Fig. 8 shows the stress-strain curve of the superplastic test of the SP700 alloy at three deformation temperatures of 700°C, 750°C, and 800°C with a constant strain rate of 0.005 s^{-1}. As seen, the yield stress decreased from 110 MPa to 63 MPa and then to 40 MPa as the test temperature increased from 700°C to 750 ℃ and 800°C. This reduction in yield stress is attributed to the activation of more slip systems at higher temperatures.

Although the yield stress of the specimen deformed at 800°C was lower than that of the one deformed at 700°C, the elongation of the specimen deformed at 700°C was higher than that of the one deformed at 800°C. Regadring to results, the maximum elongation of 1380% achieved at 700°C and constant strain rate of 0.005 s^{-1}. The elongation values obtained at 750°C and 800°C were obtained as 1000% and 1320%, respectively.

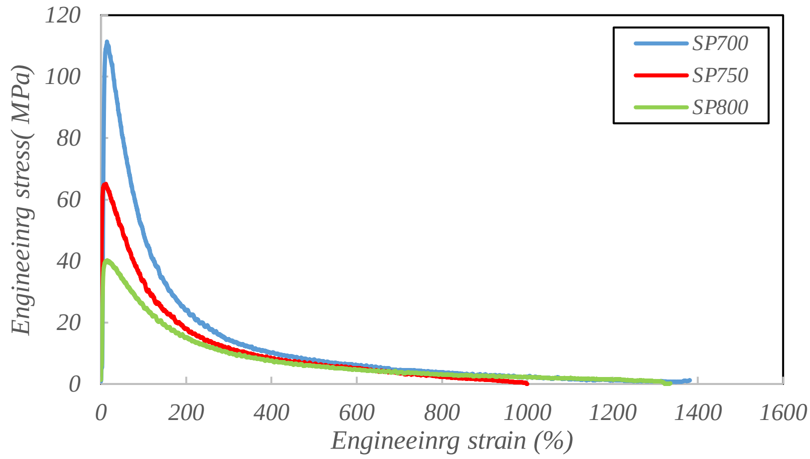

Fig. 8. The stress-strain curve of the SP700 alloy cold rolled to thickness reduction of 40% and heat treated at 700°C after superplastic test at three temperatures of 700°C, 750°C, and 800 °C and constant strain rate of 0.005 s^{-1}.

Fig. 9 shows the image and the SEM microstructure of the specimen cold rolled by thickness reduction of 40% and heat treated at 700ºC and different test tempearure of 700 to 800 ºC. The specimens exhibited high uniform elongation without necking.

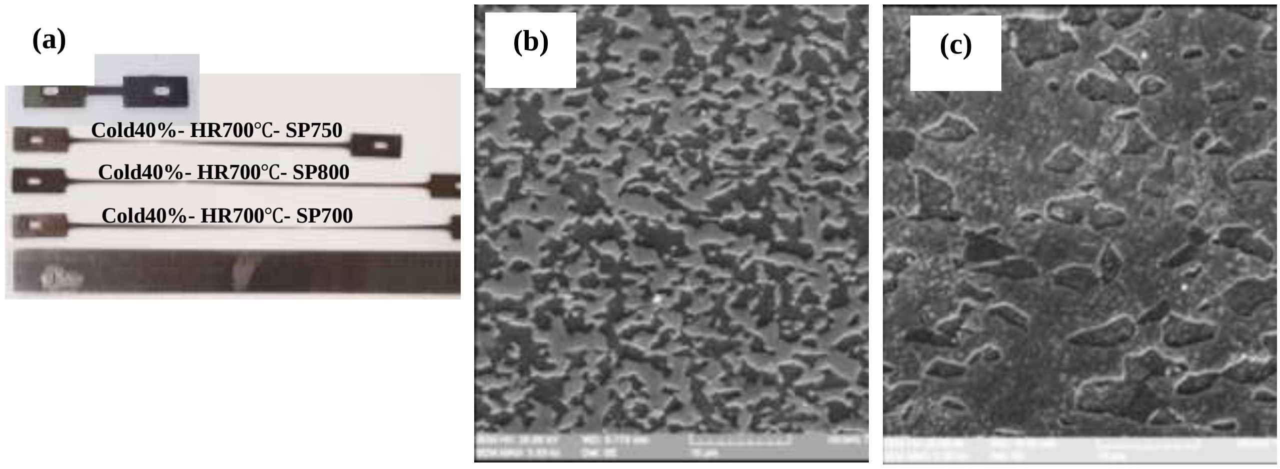

Fig. 9. (a) The image of the SP700 alloy cold rolled to thickness reduction of 40% and heat treated at 700°C after superplastic test at different temperatures and constant strain rate of 0.005 s^{-1},
(b) the SEM microstructure of the alloy after the test at 700 °C and (c) 800 °C.

As seen, the test temperature had a significant effect on the size of α phase. The average size of α phase after the superplastic test at 700ºC and 800ºC was obtained as 2.40 µm and 3.23 µm, respectively. According to the research [21], the test temperature also affected the volume fraction of α and β phases. The volume fraction of α and β phases was determined respectively as 57.7% and 42.3% for 700ºC, and 28.4% and 71.6% for 800ºC.

Another noteworthy point is the amount of lamellar structure of α phase at two different superplastic test temperature. At temperature of 700ºC, a significant amount of the α phase had a lamellar morphology. While at 800ºC, the shape of α phase changed and the semi-equiaxed coarse α phase substituted to the lamellar one.

According to studies[8], the volume fraction of the alpha phase affects the superplasticity of SP700 alloy in different ways. A higher volume fraction of the alpha phase can increase the strength and stability of the alloy, but also reduces its ductility and strain rate sensitivity. A lower volume fraction of the α phase can enhance the superplasticity of the alloy, but also make it more prone to cavitation and grain growth as the diffusion coefficient of β phase is 100 times higher than that of α phase. Therefore, an optimal volume fraction of the α phase is needed to achieve a balance between strength and ductility. The morphology of the α phase also influences the superplasticity of the SP700 alloy. The existance of lamellar α phase with equiaxed one in initial microstructure can provide suitable superplasticity as the lamellar one can increase the formation of fine spherodized α phase and consequently facilitate grain boundary sliding. However, the lamellar α phase can also cause more cavitation and damage accumulation than the equiaxed one, which can limit the superplastic deformation. Therefore, a duplex microstructure containing uniform distribution of lamellar α phase with equiaxed one is desirable for superplasticity [21, 22]. It can be speculated that the high elongation percentage achieved at 700 °C was due to dynamic recrystallization of α phase. It can be concluded that temperature is a critical factor in flow stress and superplasticity.

3.4.2. The effect of strain rate on superplasticity

The microstructure and superplastic behavior of the SP700 alloy cold rolled to 40% reduction and heat treated at 700°C was investigated by conducting tensile tests at constant temperature of 750 °C and various strain rates ranging from 0.001 s^{-1} to 0.01 s^{-1}. The engineering stress-strain curves of the alloy at different strain rates are shown in Fig. 10. The results shows that the flow stress of the alloy increased with strain rate, whereas the flow curve of it decreased with a mild behavior by decreasing the strain rate. The peak stress arised to 80 MPa and the elongation decreased to 760% by increase in the strain rate from 0.001 to 0.01 s^{-1}. The alloy exhibited a maximum elongation of 1400% and a peak stress of 30 MPa at strain rate of 0.001 s^{-1}, and the elongation of 1000% and a peak stress of 65 MPa at strain rate of 0.005 s^{-1}, as well.

According to previous studies [22,23], high strain rates prevented complete dynamic recrystallization of the microstructure. Therefore, it can be inferred that superplasticity is a phenomenon that takes place at high temperature and low strain rates.

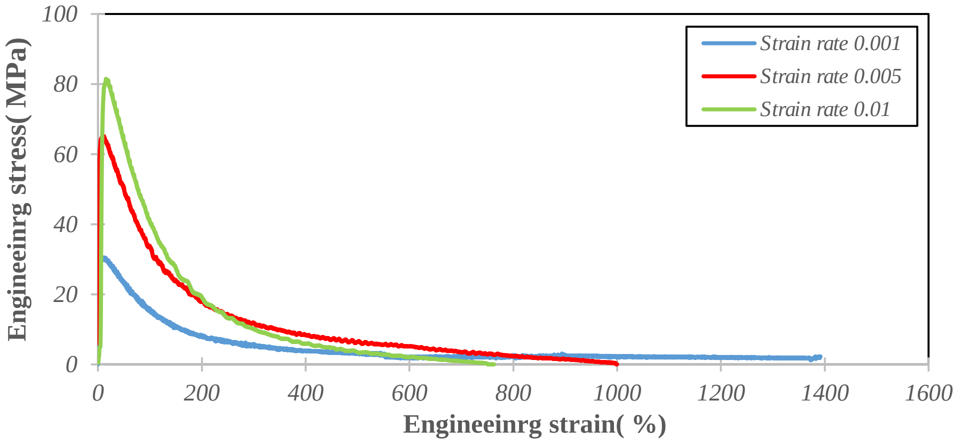

Fig. 10. The stress-strain curve of the SP700 alloy after superplastic test at strain rates of 0.01s^{-1}, 0.001s^{-1} and 0.005s^{-1} and temperature of 750°C.

3.5. Determining the superplastic deformation mechanism

The important parameters in determining the superplastic behavior of a materil are Q, m and p, respectively. Q is the activation energy or the energy required for superplastic deformation, m is the strain rate sensitivity parameter, and p is the characteristic of deformation mechanism [17]. The activation energy (Q) can be calculated from equation 1:

$$\mathrm{Ln}\dot{\varepsilon} = \mathrm{Ln}A + n.\mathrm{Ln}\,(\sinh(\alpha\sigma)) - Q/RT \qquad (1)$$

Where $\dot{\varepsilon}$ is the strain rate, A is the material constant, n is the power of stress, α is the stress exponent, and σ is the applied stress. The power of stress (n) can be obtained from the slope of Ln $\dot{\varepsilon}$-Ln (sinh (ασ)) plots at different deformation temperatures. Fig. 11(a) represents the variation of Ln $\dot{\varepsilon}$ versus Ln Sinh (ασ) at different temperatures. The slope of the mentioned plot gives the average value of a as 4.18. The activation energy (Q) was determined as 385.75 kJ/mol (Fig. 11(b)).

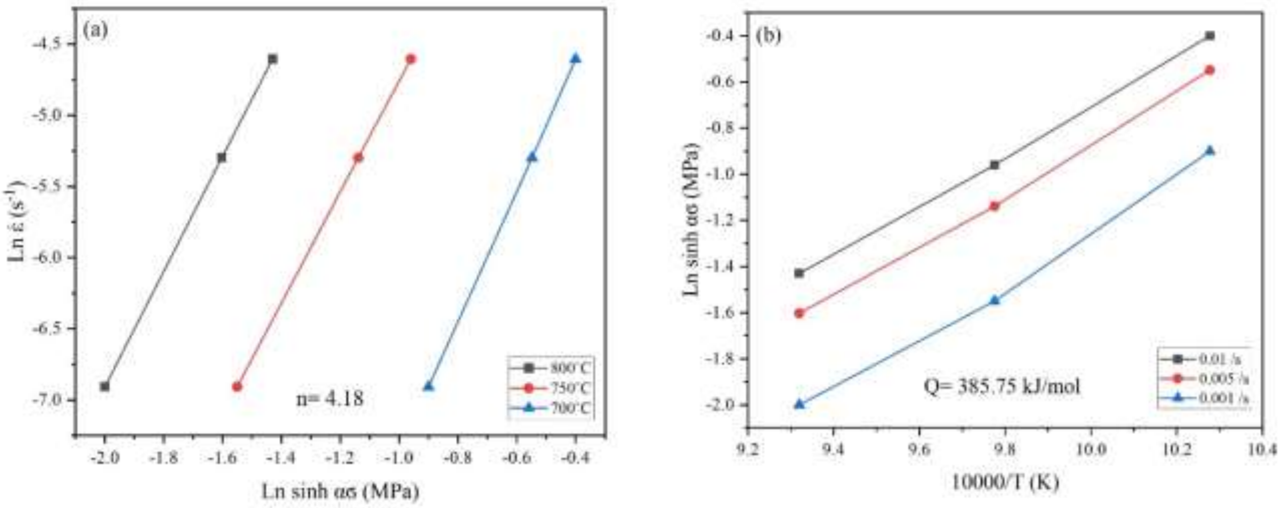

Fig. 11. The plot of (a) Ln $\dot{\varepsilon}$ versus Ln Sinh (ασ) at different temperatures and (b) the Ln Sinh (ασ) data as a function of inverse temperature at various strain rates.

The apparent activation energy reported [24] for hot deformation of the SP-700 alloy in the two phase α /β region was found to be 305.5 kJ mol^{-1},which is higher than that in the single phase β region (165.2 kJ mol^{-1}). It has been demonstrated thet the higher activation energy of deformation in two phase α /β region compared with that of single phase β region is attributed to spherodization of the lamellar α phase requiring more energy to break down the α/β interfaces. Similarly, for the alloy studied in the present work, the high activation energy of deformation can be related to the dynamic spherodization or recrystallization of the lamellar α phase (Compare Fig. 7 (a) with Fig. 7 (b)). The increase in the ductility of the alloy, as evidenced by the maximum elongation of 1400% confirmed the activation energy of 385.75 kJ/mol as a consequence of dynamic spherodization.

The strain rate sensitivity parameter (m) is one of the most important parameters for characterizing the superplastic behavior of the alloy. Superplasticity is observed when m is sufficiently high (m>0.3). The m-value can be determined from the slope of Ln σ–Ln ε̇ plot, where σ is the flow stress and ε̇ is the strain rate [18, 19].

The m-value of the alloy can be developed by the strain rate sensitivity map. For the SP-700 alloy tested in this work, the mentioned map developed at different temperatures and strain rates as shown in Figure 12. It shouudld be noted that the m values at different tempertaures and starin rates have been calculated. The 3-D map of m, strain rate and temperature has been plotted. Then, the 2-D of the 3-D manp has been plotted as Fig. 12. Regarding the map, the m value of 0.34 to 0.44 is observed as the strain rate decreased from 0.01 s^{-1} to 0.001s^{-1}. The m value changes slightly in the strain rate range of 0.01−0.005 s^{-1},with an average value of 0.39. However, in the strain rate range of 0.005−0.001s^{-1} and the temperature range of 700−730°C, the m-value became constant as 0.44.

The high m-values at low strain rates are associated with dynamic spherodization or recrystallization of the lamellar α phase, which reduces the flow stress and enhances the ductility [18]. On the other hand, researchers have shown that [25-28] the maximum m-values at low strain rates corresponds to the optimum condition for superplastic behavior, where dynamic spherodization or recrystallization contribute to grain refinement and accordingly the ductility. For diagnosing the mechanism of superplastic deformation of the alloy, the evaluation of deformation parameters such as n and p and microstructural characteristics and comparing the results with the data obtained from fundamental models developed for the alloys representing superplastic behavior is needed. The main superplastic mechanisms are grain boundary sliding accommodated by diffusion and grain boundary sliding accommodated by dislocation glide. In Table 2, the values of m, n, Q, and p obtained from the superplastic test of SP700 alloy in the temperature range of 700-800 ℃ and strain rates of 0.01-0.001 s^{-1} are presented.

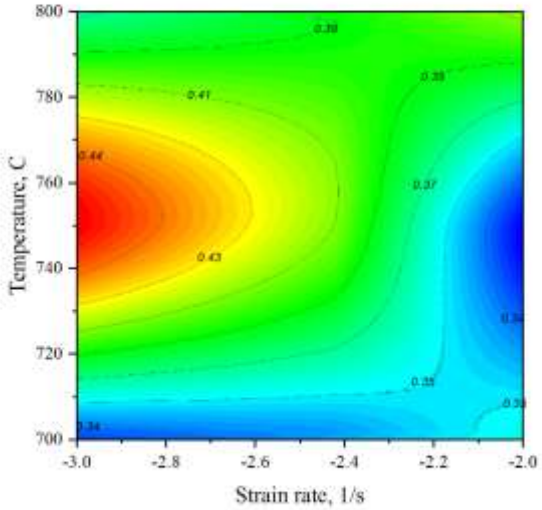

Fig. 12. The strain rate sensitivity map of the SP700 alloy during superplastic deformation.

Table 2. The results of SP700 alloy superplastic test at different temperatures and strain rates

T(°C)	$\dot{\varepsilon}$ (1/s)	m	n= 1/m	Q (kJ/mol)	p	Superplastic Mechanism
700	0.001	0.33	0.03	399.96	1.2	Rachinger
700	0.005	0.34	3.94	383.18	1.3	Rachinger
700	0.01	0.36	2.77	373.93	1.5	Rachinger
750	0.001	0.46	2.17	399.96	0.56	Rachinger
750	0.005	0.39	2.56	383.18	1.1	Rachinger
750	0.01	0.32	3.12	373.93	1.6	Rachinger
800	0.001	0.37	2.7	399.96	1.09	Rachinger
800	0.005	0.39	2.56	383.18	1.17	Rachinger
800	0.01	0.41	2.44	373.93	1.20	Rachinger

According to Table 2, possible superplastic mechanisms in this research can be dislocation slip, grain boundary slip and Ratchinger slip. Ratchinger sliding mechanism is the most probable superplastic mechanism in this research. Considering the average value of p at three superplastic temperatures of 700, 750 and 800 °C in the range of strain rates of 0.001-0.01s^{-1}, this parameter is equal to 1.33, 1.1 and 1.15, respectively.

In this research, the amount of activation energy reported as a result of the superplastic test at all the investigated strain rates and temperatures is higher than the amount of activation energy in the direction of grain boundary sliding, and this indicates grain boundary sliding to The title is superplastic mechanism. On the other hand, the obtained activation energy is higher than the creep activation energy of alpha and beta dislocations [20] , which is 306 kJ/mol and 317 kJ/mol, respectively.Considering the higher activation energy in this research compared to the activation energy of grain boundary sliding and also dislocation creep, it is predicted that the superplastic mechanism of SP700 alloy, grain boundary sliding along with dislocation matching process and the possibility of crystallization It is dynamic again.

4. Conclusions

1. The superplastic test was performed at a temperature of 800 °C and a strain rate of 0.005 s^{-1}. According to tensile evaluations, the elongation obtained from the 40 % cold-rolled at 700 °C heat treatment was 1330 %.

2. In order to reduce the superplastic test temperature and increase the strain rate in SP700 alloy, the tests were conducted at three temperatures of 700 °C and 750 °C and strain rates of 0.005 s^{-1} and 0.01 s^{-1}, which resulted in 1380 % and 760 % elongations, respectively.

3. As a result of the analysis of superplastic equations of SP700 alloy, the average value of superplastic activation energy, the range of strain rate sensitivity, and the average power of grain size was 385 kJ.mol^{-1}, 0.32-0.46, and 1.2, respectively, which proved that the superplastic mechanism was grain boundary sliding accommodate by dislocation.

References

[1] Q. Qiu, K. Wang, X. Li, J. Wang, X. Gao, K. Zhang, "Hot deformation behavior and processing parameters optimization of SP700 titanium alloy," J. Mate. Resea. Tech., Vol. 15, 2021, pp. 3078-3087.

[2] R. Boyer, G. Welsch, E.W. Collings, Materials Properties Handbook: Titanium Alloys, United States: ASM International, 1994, p. 246.
[3] E. Alabort, D. Barba, M.R. Shagiev, M,A. Murzinova, R.M. Galeyev, O.R. Valiakhmetov, A.F. Aletdinov, R.C. Reed, "Alloys-by-design: Application to titanium alloys for optimal superplasticity," Acta Mater., vol. 178, 2019, pp. 275-287.
[4] E. Alabort, D. Putman, R.C. Reed, "Superplasticity in Ti-6Al-4V: Characterisation, modeling and applications," Acta Mate., vol. 95, 2015, pp. 428-442.
[5] J. L. T. D. D. B. T. G. Z. Z. Q. Bai, "Modelling of dominant softening mechanisms for Ti-6Al-4V in steady state hot forming conditions," Mat. Sci. and Eng. A, Vol. 559, 2013, pp. 352-358.
[6] J. Luo, L.F. Wang, S.F. Liu, M.Q. Li, "The correlation between the flow behavior and the microstructure evolution during hot working of TC18 alloy," Mat. Sci. and Eng. A, Vol. 654, 2016, pp. 213–220.
[7] E. Alabort, P. Kontis, D. Barba, K. Dragnevski, R.C. Reed, "On the mechanisms of superplasticity in Ti-6Al-4V," Acta Mat., Vol. 105, 2016, pp. 449-463.
[8] S. H. Hsiang Lina, "Microtwin formation in the alpha phase of duplex titanium alloys affected by strain rate," Mat. Sci. and Eng. A, Vol. 528, 2011, pp. 2271-2276.
[9] Y. Zhang, Sh. Chang, Y. Chen, Y. Bai, C. Zhao, X. Wang, J. M. Xue, H. Wang, "Low-temperature superplasticity of β-stabilized Ti-43Al-9V-Y alloy sheet with bimodal γ-grain-size distribution," J. . Sci. Tech., Vol. 95, 2021, p. 225–236.
[10] J. Shen, Y. Sun, Y. Ning, H. Yu, Z. Yao, L. Hu, "Superplasticity induced by the competitive DRX between BCC beta and HCP alpha in Ti-4Al-3V-2Mo-2Fe alloy," Mate. Charac., Vol. 153, 2019, pp. 304–317.
[11] AMS 4899C, "Titanium Alloy, Sheet, Strip, and Plate Ti-4.5Al-3V-2Fe-2Mo Annealed," 2011.
[12] AMS 4964C, "Titanium Alloy Bars, Wire, Forgings, and Rings Ti-4.5Al-3V-2Fe-2Mo Annealed," 2011.
[13] ASTM E8/E8M-13, Standard Test Methods for Tension Testing of Metallic Materials, West Conshohocken: ASTM International, 2013.
[14] F. a. M.Hatherly, Recrystallization and Related Annealing Phenomena, Elsevier, 2004. p. 245.
[15] Y. W. S. X. H. S. Tian N, " Microstructure and Texture Evolution during Superplastic Deformation of SP700 Titanium Alloy," Mater., Vol. 15, No. 5, 2022, 1808.
[16] Z. W. M. L. Z. P. H. B. Piao R, "Characterization of Hot Deformation of near Alpha Titanium Alloy Prepared by TiH2-Based Powder Metallurgy," Mater., Vol. 15, No. 17, 2022, 5932.
[17] . Zener, J.H. Hollomon, "Effect of Strain Rate Upon Plastic Flow of Steel," J. Appl. Phy., Vol. 15, 1994, pp. 22-32.
[18] K.A. Padmanabhan, R.A. Vasin, F.U. Enikeev, "Superplastic Flow, Phenomenology and Mechanics", Springer-Verlag Berlin Heidelberg, New York, 2001.
[19] M.J.Tan, G.W.Chen, S.Thiruvarudchelvan, "High temperature deformation in Ti–5Al–2.5Sn alloy," J. Mater. Proc. Tech., Vol. 192-193, 2007, pp. 434-438.
[20] M. Meier, D. Lesuer, A. Mukherjee, "The effects of the α/β phase proportion on the superplasticity of Ti-6Al-4V and iron-modified Ti-6Al-4V," Mat. Sci. and Eng. A, Vol. 154, 1992, pp. 165-173.
[21] I. Balasundar, T. Raghua, P. Kashyap, "Modeling the hot working behavior of near-α titanium alloy IMI 834," Progress in Natural Science: Materials International, Vol. 23, 2013, pp. 598-607.
[22] P. Wanjara, M. Jahazi, H. Monajati, S. Yue, J.P. Immarigeon, "Hot working behavior of near-α alloy IMI834," Mat. Sci. and Eng. A, Vol. 396, 2005, pp. 50-60.
[23] Z. Ma, R. Mishra, Friction Stir Superplasticity for Unitized Structures, Butterworth-Heinemann, 2014, p. 39-57.
[24] Q. Yang, K. Qiu, R. Jiang, D. Huang, "Characterization of Hot Deformation Behavior of TC18 Titanium Alloy," Mat. Sci. For., Vol. 815, 2015, pp. 263-267.
[25] L.W. Zhu, X.N. Wang, Y. Fei, J. Li, Z.Sh. Zhu, "Characterization of hot deformation behavior of Ti-4.5Al-3V-2Mo-2Fe titanium alloy," Mat. Sci. For., Vol. 849, 2016, pp. 309-316.
[26] A. H. Sheikhali, M. Morakabati, S. M. Abbasi, "Hot torsion behavior of SP-700 near beta titanium alloy in single and dual phase regions" Inte. J..Mate. Resea., Vol. 109, no. 12, 2018, pp. 1136-1145.
[27] M. J. Tan, G.W. Chen, S. Thiruvarudchelvan "High temperature deformation in Ti–5Al–2.5Sn alloy," J. Mat. Proc. Tech., Vols. 192-193, 2007, pp. 434-438.
[28] V.G. Krishna, Y.V.R.K. Prasad, N.C. Birla, G.S. Rao, "Processing map for the hot working of near-α titanium alloy 685," J. Mat. Proc. Tech., Vol. 71, 1997, pp. 377-383.